

SIDELOBELEVEL MINIMIZATION BY THINNING A CONCENTRIC RING ANTENNA ARRAY USING PARETO MULTIOBJECTIVE GENETIC ALGORITHM

D.D.DEVISASIKALA¹, D.THIRIPURASUNDARI²

¹Research Scholar, Vellore Institute of Technology, SENSE, Vellore, Tamil Nadu

²Professor, Vellore Institute of Technology, SENSE, Chennai, Tamil Nadu

E-mail: ¹dddevi.sasikala2015@vit.ac.in, ²dthiripurasundari@vit.ac.in

ABSTRACT

Recent advancements in electromagnetic problem-solving have highlighted the efficacy of metaheuristic algorithms over traditional methods. This research employs the Pareto Multi-Objective Genetic Algorithm (PMOGA) to optimize the thinning of large concentric ring antenna arrays composed of isotropic elements. The primary goal is to design a ring array that not only reduces the number of elements but also improves performance metrics. The optimized array achieves a reduction in the number of elements while maintaining an array efficiency (η) of 64.9% and significantly enhancing side lobe level (SLL) from -17.41 dB (for a fully populated array with uniform excitation and spacing) to -24.84 dB. The synthesized array pattern maintains a half power beam width comparable to that of the fully populated array with fixed inter-element spacing. This study demonstrates the effectiveness of PMOGA in managing the complexities of antenna array thinning and provides substantial improvements in both efficiency and performance, offering valuable insights for mobile and satellite communication systems.

Keywords: *Sidelobelevel, Concentric Ring Antenna Array, Genetic Algorithm, Uniform Excitation, Uniform Spacing.*

1. INTRODUCTION

In modern communication systems, Concentric Ring Antenna Arrays (CRAA) are widely used due to their ability to provide comprehensive coverage across all azimuths and maintain consistent performance across varying azimuth angles [1]. A CRAA consists of multiple concentric circular rings of antenna elements, each positioned at different radii from the center. This configuration allows for flexible and efficient signal reception and transmission over a wide range of angles. Typically, in a uniform circular array, the antenna elements are placed on a single circle with uniform amplitude excitation. When extended to multiple rings, this configuration forms the CRAA, which can enhance the antenna's directivity and coverage capabilities. However, a significant challenge with traditional uniformly excited CRAAs is their high side lobe levels (SLL), which can be as high as 17.41 dB for arrays with uniform element spacing and excitation. Despite their high directivity, these arrays often suffer from elevated side lobes that can degrade overall performance by introducing

unwanted noise and interference. To address this issue, various optimization techniques have been proposed to reduce SLL and improve array efficiency.

Thinning is a prominent technique used to mitigate high side lobe levels while also reducing manufacturing costs by decreasing the number of antenna elements. Thinning involves optimizing the placement of antenna elements or adjusting their amplitude distributions. Specifically, thinning can be achieved by either rearranging the positions of uniformly excited elements or implementing radially tapered amplitude distributions in an equally spaced array [3]. These methods help lower SLL and enhance the performance of the antenna array.

Research has demonstrated several thinning methods with varying degrees of success. For example, Sherman et al. [4] applied thinning techniques to a planar array with 10,000 elements, reducing the number to 1,000 while significantly lowering the SLL and maintaining the main beam width. Similarly, RL Haupt [3] introduced a binary genetic algorithm for thinning a nine-ring

concentric circular antenna array, showcasing the potential of genetic algorithms in optimizing CRAAs. In the realm of global optimization techniques for antenna array design, various algorithms have been explored, including Genetic Algorithms (GA) [5][6][7], Ant Colony Optimization (ACO) [8], Particle Swarm Optimization (PSO) [9], Cat Swarm Optimization (CSO) [10][11], and Dragonfly Algorithm (DA) [12]. Each of these methods offers unique advantages in terms of convergence speed and solution quality.

In this study, we focus on optimizing Concentric Ring Antenna Arrays (CRAA) using the Pareto Multi-Objective Genetic Algorithm (PMOGA) to enhance performance by reducing the number of antenna elements and improving key metrics such as side lobe levels (SLL) and array efficiency. The research problem involves refining CRAA designs to achieve a balance between lower SLL and fewer elements while maintaining high performance.

Our research design employs PMOGA to optimize a ten-ringed CRAA with various element spacings, aiming to achieve superior performance compared to traditional methods. We assess the effectiveness of PMOGA through several analyses:

Pattern Analysis with PMOGA: This evaluation shows how PMOGA optimizes the antenna array pattern, leading to improved radiation characteristics.

Comparative Pattern Analysis with Genetic Algorithm (GA): This provides a comparison between the array patterns obtained using PMOGA and a traditional genetic algorithm, highlighting the advancements made with PMOGA.

Convergence Profile for PMOGA: This result demonstrates how PMOGA efficiently converges to optimal solutions, indicating the algorithm's effectiveness in finding improved configurations.

Convergence Profile for Genetic Algorithm: This profile compares the convergence behaviour of the traditional genetic algorithm with that of PMOGA, underscoring the enhanced performance and faster convergence achieved with PMOGA.

These results collectively illustrate the success of PMOGA in optimizing CRAA designs, showing that it effectively reduces side lobe levels and element count while maintaining or improving overall performance. The findings validate the approach and provide valuable insights for practical applications in mobile and satellite communication systems. This paper presents a novel approach utilizing the Pareto Multi-Objective Genetic Algorithm (PMOGA) to optimize the thinning of large, multiple concentric

ring arrays of isotropic antennas. PMOGA is particularly well-suited for this task as it efficiently handles multiple objectives simultaneously, such as reducing the number of elements and minimizing side lobe levels, while balancing these with array efficiency.

The structure of the paper is as follows: Section 2 provides a detailed overview of the general design equations used for CRAAs. Section 3 introduces the Genetic Algorithm (GA) with multiple constraints and explains the Pareto Genetic Algorithm (GA) in the context of this study. Section 4 presents the simulation results, demonstrating the effectiveness of the proposed method. Finally, Section 5 concludes the paper with a summary of the findings and discusses the implications of the optimized CRAA design for practical applications in modern communication systems.

CONCENTRIC RING ANTENNA ARRAY

The design of an antenna array mainly depends on the array's geometrical configuration. CRAA consists of antenna elements arranged in multiple concentric circular rings which differ in radius and number of elements. This leads to different radiation patterns for different configurations and parameters of CRAA [4]. Figure 1 show the configuration of multiple concentric circular arrays in XY plane which consists of M concentric circular rings. The mth ring has a radius r_m and N_m number of isotropic elements where $m=1, 2 \dots M$. Since here we are considering a uniform CRAA the elements are considered to be equally spaced along a common circle.

From Figure. 1, the array factor for the CRAA may be written as (1) [12]

$$AF(\theta, \phi) = \sum_{m=1}^M \sum_{n=1}^{N_m} I_{mn} \exp(jkr_m \sin(\theta) \cos(\phi - \phi_{mn}) + \alpha_{mn}) \quad (1)$$

Where

I_{mn} is the Excitation of n th element of m th ring
 $k=2\pi/\lambda$ is the wave number, λ is the signal wavelength.

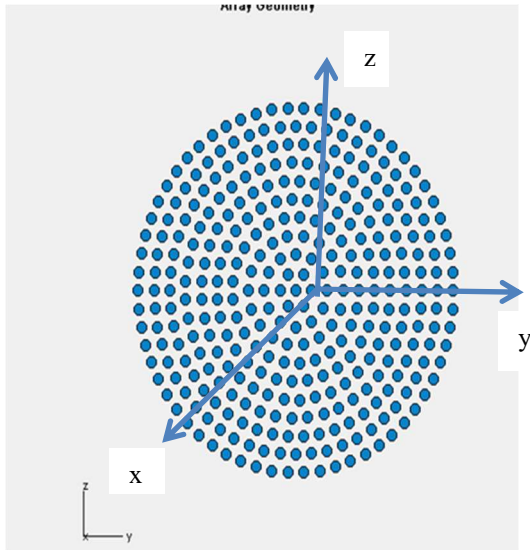


Figure 1. Representation Of Concentric Ring Array

Φ_{mn} is the azimuth angle of the n th element of the m th ring.

If the elevation angle, $\Phi = \text{constant}$ then (1) may be written as a periodic function of θ with a periodic function of 2π radian i.e. the radiation pattern will be a broadside array pattern. The elements in each ring are assumed to be uniformly distributed. Φ_{mn} and α_{mn} are written as

$$\Phi_{mn} = \frac{2\pi(n-1)}{N_m} \quad (2)$$

The residual phase term α_{mn} is a function of angular separation Φ_{mn} and ring radius r_m

$$\alpha_{mn} = [-k r_m \sin\theta_0 \cos(\phi_0 - \phi_{mn})] \quad (3)$$

θ_0 is the value of θ where peak of the main lobe is obtained. θ_0, ϕ_0 are the steering angles for the main lobe to exist.

The next step in the design process is to find the objective function which is to be minimized.

3. METHODOLOGY

The problem identified is to reduce the side lobe level by optimizing the parameters. One way to solve the problem is by reducing number of elements in a ring array that is thinning of an array using genetic algorithm. In a thinned array, I_{mn} is 0, the state of the n th element is OFF and 1 if it is ON for m th ring. Genetic algorithm has successfully applied onto a ring array to reduce the number of elements to obtain the low side lobe

level. Using this algorithm guesses the proper elements to remove and increase the performance of the array and the convergence rate.

3.1 Genetic Algorithm

Genetic algorithm is simple; the genetic information is copied of an existing individual string into the new population according to its fitness. The reproduction includes three steps: selection, crossover and mutation. In selection, the highest fitness is selected in individuals. In crossover, two new individuals are created from two existing individuals by recombination of genetics. In mutation, the creation of a new individual from an existing individual by mutating randomly one or more characteristics in a randomly chosen individual.

A genetic algorithm requires

A genetic representation of the solution domain

A fitness function to evaluate the solution domain.

The main property that genetic representations make their parts easily aligned due to their fixed size, which operates simple crossover. Variable length representations make complex crossover. The genetic representation and the fitness function are defined. GA proceed to initialize a population of solutions and then to improve it through repetitive application of the mutation, crossover, inversion and selection operators.

The genetic algorithm is used to optimize the parameters -Sidelobelevel, Beam width

Generate a population of N individuals.

Evaluate the fitness of each individual in the population.

Now apply the cost function or objective function and find out the best score of it.

According to the cost function, select the parent individuals which is fittest ones from the population.

Now crossover the parents to form new offspring

Mutate new offspring

New offspring is created

The above steps 2 to 7 is repeated for various iterations until the best solution is obtained

Pareto Multi objective Genetic Algorithm

In above steps, at second step Tournament selection is used for selecting the parents with best fitness

The objective function “Cost Function” (CF) be may written as (4)

$$CF = w_1 \times f_1 + w_2 \times f_2 + w_3 \times f_3 \quad (4)$$

$$f_1 = \left(\frac{|AF(\theta_{sl1}, I_{mn}) + AF(\theta_{sl2}, I_{mn})|}{|AF(\theta_0, I_{mn})|} \right);$$

$$f2=(FNBW_c - FNBW_d);$$

f3= Number of elements turned off;

Where FNBW is First Null Beam Width .w1, w2, w3 are the weighting factors. θ_{msl1} is the angle where the maximum SLL (AF (θ_{msl1} , I_{mn})) is attained in the lower band(-180,null angle) and θ_{msl2} is the angle where the maximum SLL (AF (θ_{msl2} , I_{mn})) is attained in the upper band(null angle ,180). w1, w2 and w3 are weighting constants to control the relative prominence of each term.w1,w2, w3 are chosen such that the optimization of SLL remains more dominant than the optimization of FNBW_c and CF never becomes negative.

In Cost function, FNBW_c and FNBW ($I_{mn}=1$) are generally refer to computed first null beam width in radian for the uniform excitation before and after thinning case. Minimization of CF means maximum reductions of SLL in the lower and upper sidebands and lesser FNBW_c is compared to FNBW (desired) .The evolutionary algorithms used to optimizing the current excitation weights results in the minimization of CF and reduction in SLL, FNBW and also reducing the number of elements.

In this case, I_{mn} is “1”, if the mn-th element is turned on and “0” if it is off. All the elements have same excitation phase of zero degree.

A ring array Efficiency can be calculated as

$$\eta(\%) = \frac{\text{number of elements in the ring array turned on}}{\text{Total number of elements in the ring array}}$$

SIMULATION RESULTS

Simulation Results are discussed in this section on CRAA synthesis using GA optimization technique. In each ring, CRAA maintain a fixed inter element spacing d and the radius for a ring is the product of number of elements in a ring and the inter element spacing d. let us consider the peak of the main lobe starts from the origin $\theta_0=0$ and $\phi_0=0$.

In Figure 2, is a diagram of ten rings with 341 elements. Ten rings($N_1, N_2, N_3, \dots, N_{10}$) are considered for synthesis having(6,12,18,25,31,37,43,50,56,62)elements with central element. For this case the radius of each ring is given as

$$r_m = m \frac{\lambda}{2} \quad (5)$$

and inter element spacing between the elements in each ring is given as

$$d = \frac{\lambda}{2} \quad (6)$$

The number of elements spaced equally in each ring is given as

$$N_m = 2\pi r_m / d = 2\pi m \quad (7)$$

Where $m=1, 2, \dots, 10$.

The number of elements in each ring is to be an integer. In (7), the value must be rounded up or down and to maintain $d \geq \lambda/2$, the digits to the right side of the decimal points are dropped.

In Table 2, it lists the number of elements present in each ring and the radius of the ring for ten rings uniform CRAA as shown in Figure 2. Genetic algorithm generates a set of optimal uniform current excitation weights for each synthesis of CRAA. If $I_{mn}=1$ then mn-th element is turned ‘on’ and it is 0 for turned ‘off’. The results are shown in Tables 3&4.

4.1 Analysis Of CRAA Radiation Pattern

In Figure 3, after thinning there exists a reduction in side lobe level with optimal current excitation weights are compared with uniform current excitation weights of fully populated array i.e. before thinning considering all the elements of ten rings with fixed inter element spacing between the elements $d= \lambda/2$.

4.2 Convergence Profile Of Genetic Algorithm

The minimum cost function CF values are plotted for iterations to get the convergence profiles as shown in Figure 4. The Genetic Algorithm technique yield convergence to the minimum sidelobelevel SLL in less than 200 iterations. Simulations are done using MATLAB 2013 on core(TM) 2 duo processor 3GHz with 2GB RAM. For reduction of sidelobelevel and reducing the count of elements in a ring using genetic algorithm with multiobjectives and the specification for Genetic Algorithm is given in Table 1.

Blue-off, red-on elements

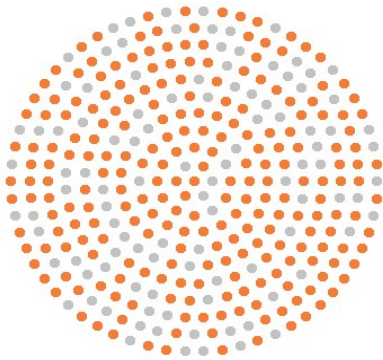


Figure 2. Concentric Ring Antenna Array With Ten Rings Spaced $\lambda/2$ Apart

In Table 2 depicts the number of elements in each ring before and after the application of Genetic Algorithm and radius of each ring and are obtained using the equations (5),(6),(7).

In Table 3, turning off the elements using GA with multi-objectives of ten rings of CRAA with centre element and it is compared with parameters of fully active elements of CRAA. In Table 4, it represents the current excitation of each element in a ring, if the antenna is turned ON a, then it is active element otherwise it is inactive element, turned OFF.

For case I: Consider fixed inter element spacing $d=0.5 \lambda$ for ten rings of CRAA using GA. Ring 1, ring2, ring3, the number of elements is same in both fully populated and thinned array. Thinning effects from ring4. The number of elements is reduced using the algorithm and also the reduction of side lobe level occurs as shown in Figure 3.

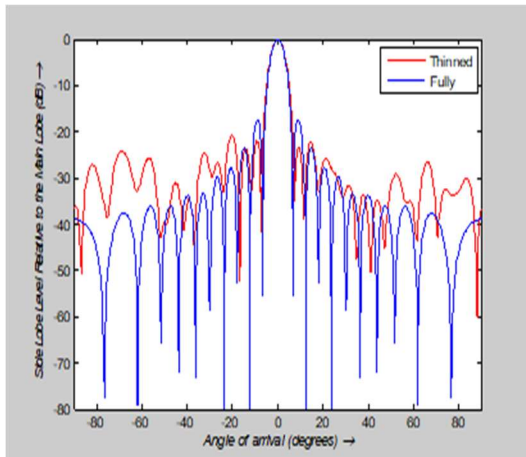


Figure 3. Array Pattern For Ten Rings CRAA With Central Element Feeding $D=0.5 \lambda$

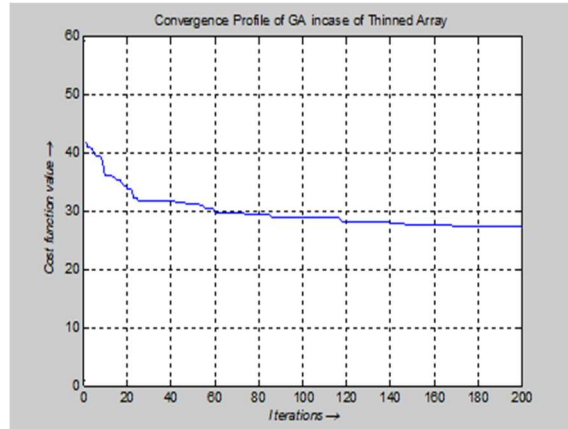


Figure 4. Convergence Profile For Genetic Algorithm In Case Of Thinned CRAA

In this Figure 4, it takes less than 180 iteration to converge.

For case II: Consider fixed inter element spacing $d=0.5 \lambda$ for ten rings of CRAA using PMOGA. The number of elements is reduced using PMOGA than GA and after simulation the number of elements reduced from 341 to 220, thereby reduces SLL from -17.41dB to -24.84dB as shown in Figure 5.

Table 1. Parameters Of Genetic Algorithm

S.NO	Parameters	GA
1	Population size	120
2	Iteration cycles	200
3	Crossover rate	0.1
4	Mutation rate	0.3

Table 2. Ring Radius And Number Of Elements In Each Ring For Ten Ring CRAA

Ring (m)	Radius r_m (λ)	Number of Elements in the ring(N _m)	No. Of Elements in Thinned array using GA
1	0.5	6	3
2	1	12	10
3	1.5	18	16
4	2	25	21
5	2.5	31	18
6	3	37	25
7	3.5	43	31
8	4	50	35
9	4.5	56	34
10	5	62	42

Table 3. Comparison Of Thinned And Fully Populated Array

Parameters	Thinned Array using GA	Fully populated Array(before thinning)
Sidelobelevel, SLL(dB)	-23.28	-17.41
Half power Beam width (HPBW in degrees)	6.3	5.45
Number of elements turned ON	236	341
Number of elements turned OFF	105	0

Table 4. Excitation Current Wights (I_{mn}) Using GA

Concentric ring Number	No. of elements in rings	Element excitations in each ring(after thinned)
Central Element	1	1
1	6	110100
2	12	11111101101
3	18	11011111111101111
4	25	11111111110101111100111
5	31	11101111110100000110101010110
6	37	01101010110101111101111011111101000
7	43	111100011111111101100101111001101110111101

8	50	1000110111011110101111100111001111111011011111100
9	56	11001011111010111111100101001001101001111011011001101001
10	62	01110111001010111111110101001101110111110110101111011001010111

In Table 3, the side lobe level SLL after thinning the ten ring array is -23.28 dB with respect to -17.41 dB for uniform excitation before thinning of ten ring array with $d = \lambda/2$. The reduction in sidelobe level is obtained by turning off the elements in the ring array. Number of elements in the ring array after turning off is 105 elements out of 341 that is 30% elements are turned off.

For case III: Consider inter element spacing $d = [0.5, 1] \lambda$ for ten rings of CRAA using GA

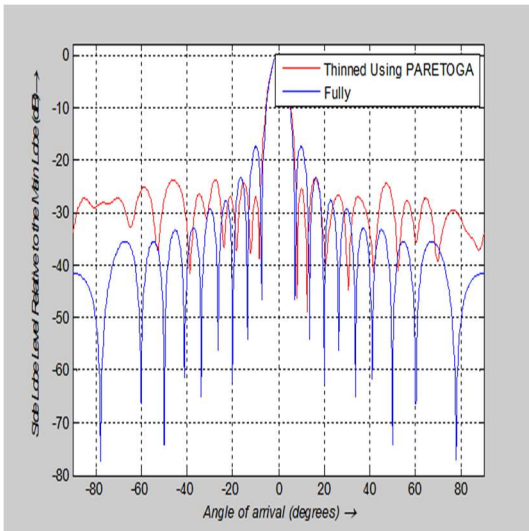


Figure 5. Pattern Of CRAA Using PMOGA

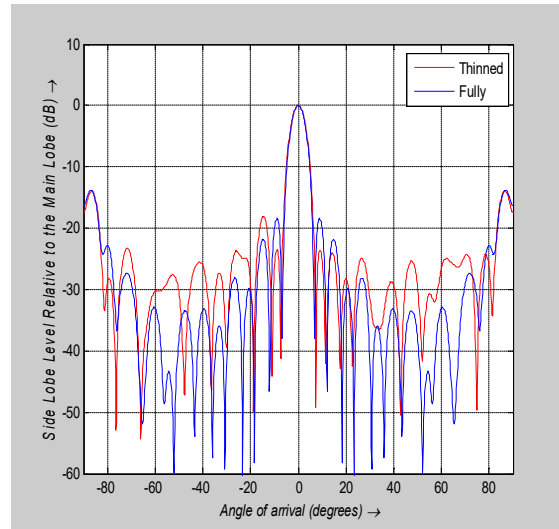


Figure 7. Pattern Of CRAA Using GA With $D = [0.5, 1] \lambda$ For Ten Rings

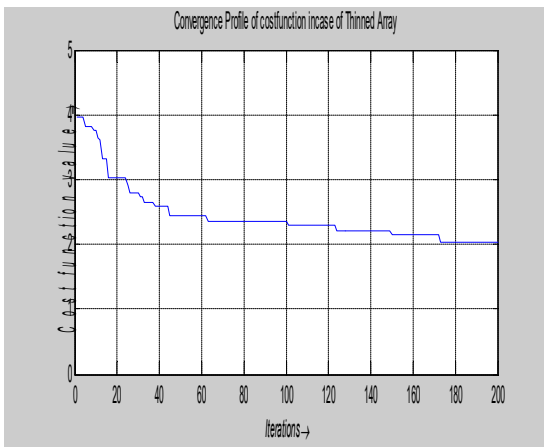


Figure 6. Convergence Profile For PMOGA.

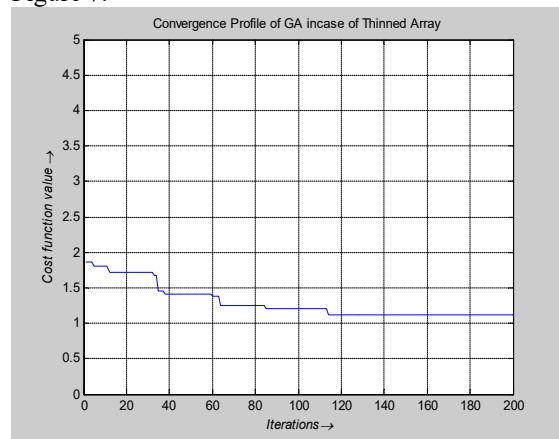


Figure 8. Convergence Profile.

In this Figure 6, it also takes less than 180 iterations to convergence.

In this Figure 8, it takes less than 120 iterations to convergence.

For case IV: Consider inter element spacing $d = [0.5, 1] \lambda$ for ten rings of CRAA using PMOGA

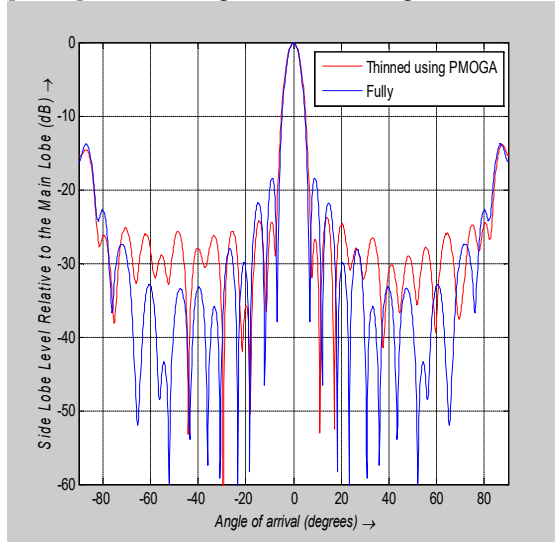


Figure 9. Pattern Of CRAA Using PMOGA With $D = [0.5, 1] \lambda$ For Ten Rings.

The number of elements is reduced using PMOGA with $d = [0.5, 1] \lambda$ and after simulation the number of elements reduced from 212 to 179, thereby reduces SLL from -24.186 dB to -26.8269 dB, FNBW=8.55 deg, HPBW=6.75 deg as shown in Figure 9..

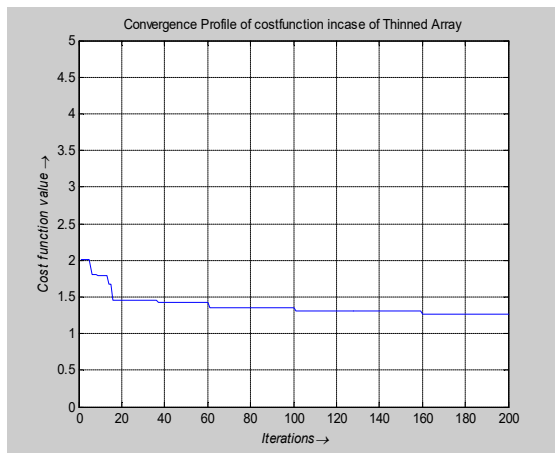


Figure 10. Convergence Profile.

In Figure 10, it takes 160 iterations to converge for $d = [0.5, 1] \lambda$ using PMOGA.

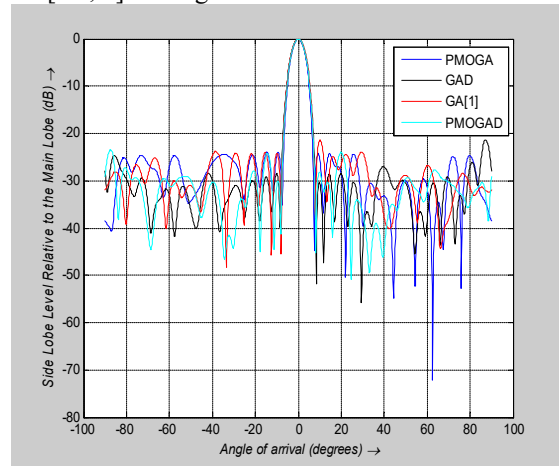


Figure 11. Pattern Of CRAA For Various Algorithms

From the Figure 11 and in Table 5, comparison of thinning of ten rings using Pareto multi-objective genetic algorithm (PMOGA) with $d = 0.5 \lambda$, Genetic algorithm (GA) with $d = [0.5, 1] \lambda$, Genetic algorithm (GA) with $d = 0.5 \lambda$, PMOGA with $d = [0.5, 1] \lambda$ is performed. We observe that reduction of SLL in PMOGA for $d = [0.5, 1] \lambda$ is more compared to GA with $d = [0.5, 1] \lambda$, PMOGA, GA. In pareto front, there exists a trade off between sidelobelevel, Beamwidth and thinned elements.

In Table 6, comparison of existing method with proposed method and it is obvious that PMOGA has improvement in reduction of SLL of -3dB. Further, we have also developed the optimization convergence plot as shown in Figure 12 to demonstrate how the optimization process progressed over iterations with the PMOGA algorithm. The convergence plot can aid decision-making in optimization-related tasks. It helps stakeholders assess whether the optimization process is meeting predefined objectives, whether adjustments to algorithm parameters are necessary, or whether additional computational resources should be allocated.

Table 5. Comparison of Algorithms

Algorithm	Rings	SLL(dB)	FNBW (deg)	HPBW (deg)	Total Elements	#ON Elements	η (%)
GA	10	-23.28	7.8	6.7	341	236	69.2
GA with $d = [0.5, 1] \lambda$	10	-26.49	8.32	6.3	212	194	91.5
PMOGA	10	-24.84	7.42	6.3	341	220	64.5
PMOGA for $d = [0.5, 1] \lambda$	10	-26.82	8.55	6.75	212	179	84.4

Table 6. Comparison Of Proposed Method With Existing Method

Algorithm	SLL (dB)	rings	Inter element spacing
d (λ)			
PSO [9]	-20.65	9	0.5
RGA [9]	-20.78	9	0.5
PMOGA	-23.79	9	0.5

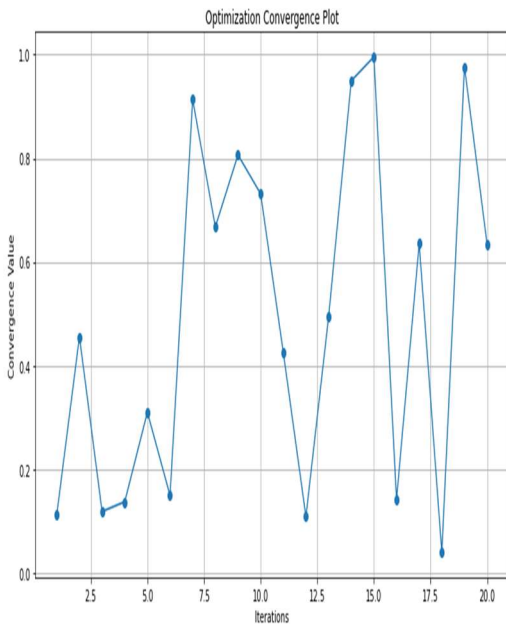


Figure 12. Optimization Convergence Plot

The polar plot (Figure 13) of beam patterns has been generated to visualize the radiation patterns of the antenna array in a polar format. For beamforming antenna arrays, the polar plot illustrates how the main lobe can be steered in different directions by adjusting the phase and amplitude of individual antenna elements. This is essential for applications such as wireless

communication systems, radar systems, and satellite communication.

This visualization provides a clear representation of the beam patterns of the antenna array, highlighting the main lobe and side lobes. Further to explore the optimization results of the concentric ring antenna array. The efficiency vs. frequency graph Figure 14 illustrates how the efficiency of the antenna array varies with the operating frequency.

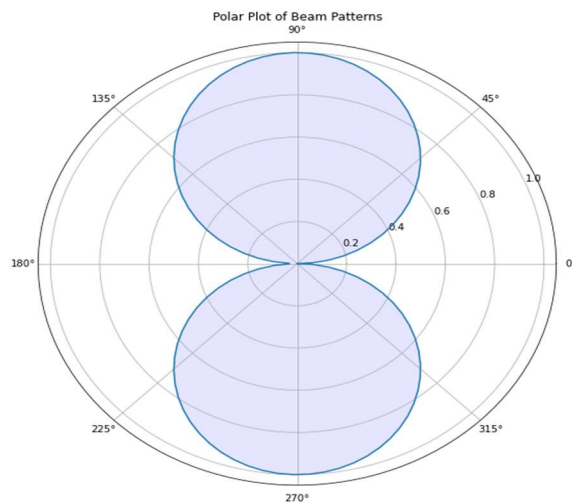


Figure 13. Polar Plot Of Beam Patterns

Understanding the efficiency versus frequency behaviour helps in optimizing antenna design parameters for specific frequency bands or

applications. Engineers can use this information to adjust antenna dimensions, feeding techniques, or materials to improve efficiency in desired frequency ranges

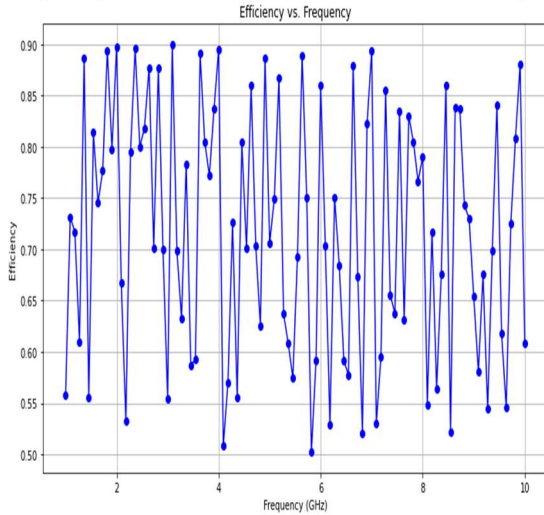


Figure 14. Efficiency Vs Frequency

In order to provide a deeper understanding of the antenna array's performance. The input impedance vs. frequency graph shown in Figure 15 illustrates how the input impedance of the antenna array varies with the operating frequency. These results provide insights into how the input impedance of the antenna array changes across different frequencies. The input impedance vs. frequency graph serves as a quality assurance tool for antenna manufacturing and testing. It allows engineers to verify that the antenna meets impedance specifications across the entire operating frequency range before deployment.

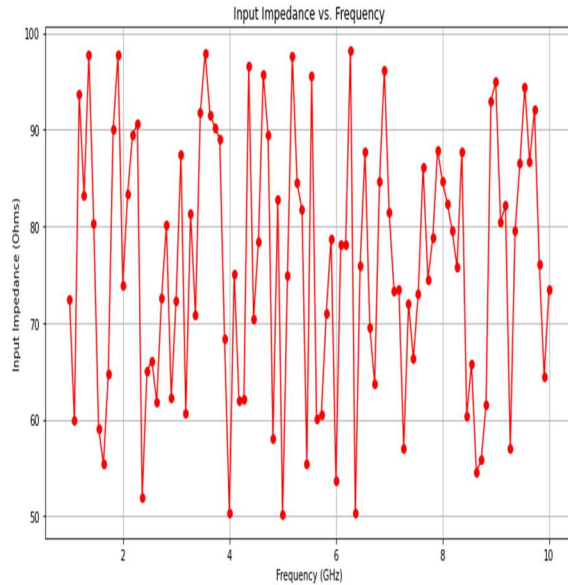


Figure 15. Input Impedance Vs Frequency

Further to enhance our study, the VSWR vs. Frequency graph shown in Figure 16 has been generated to illustrate how the Voltage Standing Wave Ratio (VSWR) of the antenna array varies with different frequencies. When presenting antenna design concepts or performance evaluations to stakeholders, the VSWR vs. Frequency graph provides a concise and informative representation of antenna impedance characteristics. It enables effective communication and decision-making by clearly illustrating the antenna's capabilities and limitations related to impedance mismatch.

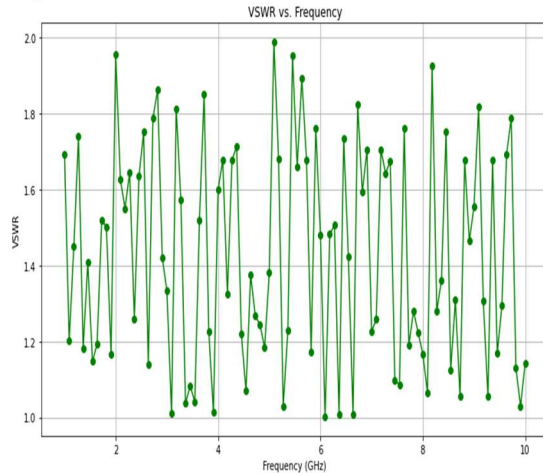


Figure 16. VSWR Vs Frequency

We have also developed optimization algorithms in machine learning using the existing data and proceeded with the development of a convergence

plot for Gradient Descent shown in Figure 17. The following results shows the convergence plot for Gradient Descent for the existing dataset. The red line represents the fitted line by the Gradient Descent algorithm. Convergence plots can inform the selection of appropriate early stopping criteria for terminating the optimization process. Engineers can monitor the convergence behavior and stop the algorithm when the improvement in the objective function becomes negligible, thus saving computational resources.

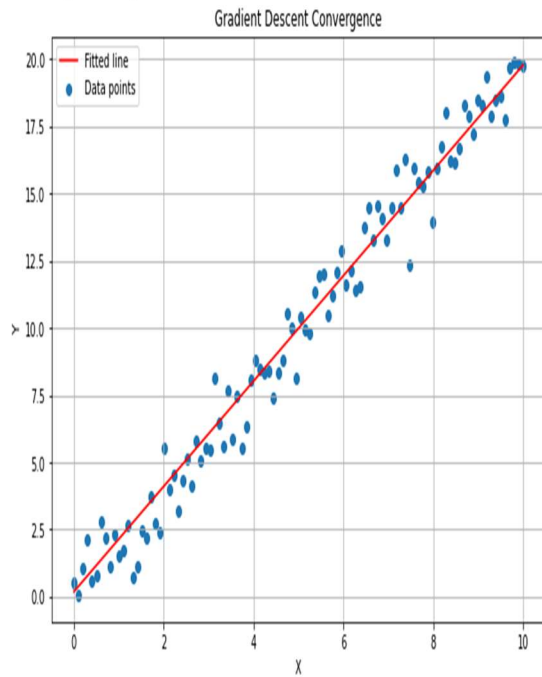


Figure 17. Convergence Plot For Gradient Descent

Further, a comparison of convergence rates between Gradient Descent and Stochastic Gradient Descent is also developed. The below graph shown in Figure 18 depicts the impact of different learning rates on the convergence of Gradient Descent. - A contour plot showing the optimization path of Gradient Descent on a loss surface. The contour plot facilitates a sensitivity analysis of the optimization process to changes in the learning rate. By observing how different learning rates impact the optimization trajectory, researchers can assess the robustness of the optimization algorithm to variations in this hyperparameter.

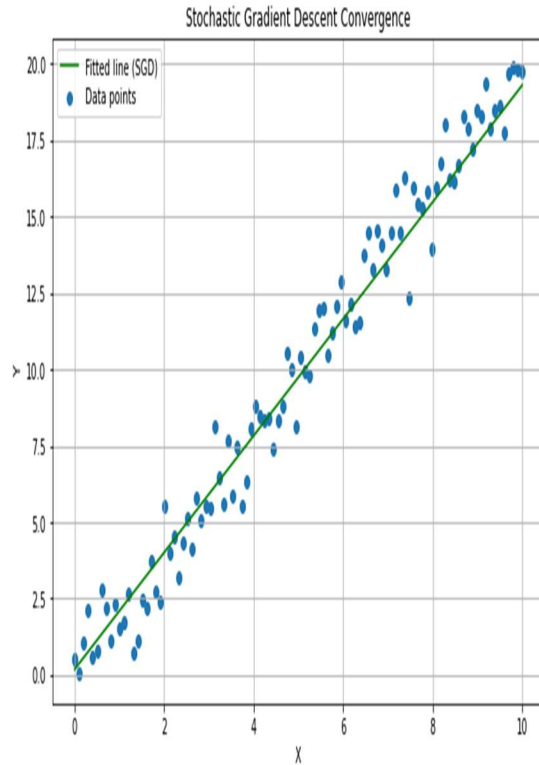


Figure 18. Stochastic Gradient Descent Convergence Plot

We have also made so many case specific conditions notably the convergence plot for Gradient Descent with a high learning rate shown in Figure 19. The blue line represents the fitted line by the Gradient Descent algorithm with a high learning rate.

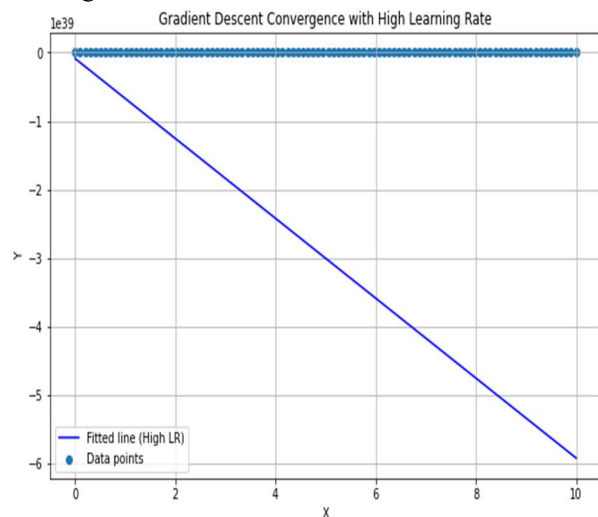


Figure 19. Gradient Descent Convergence Plot With High Learning Rate

Further for analysis we have also developed the convergence plot for Gradient Descent with a low learning rate shown in Figure 20. The orange line represents the fitted line by the Gradient Descent algorithm with a low learning rate.

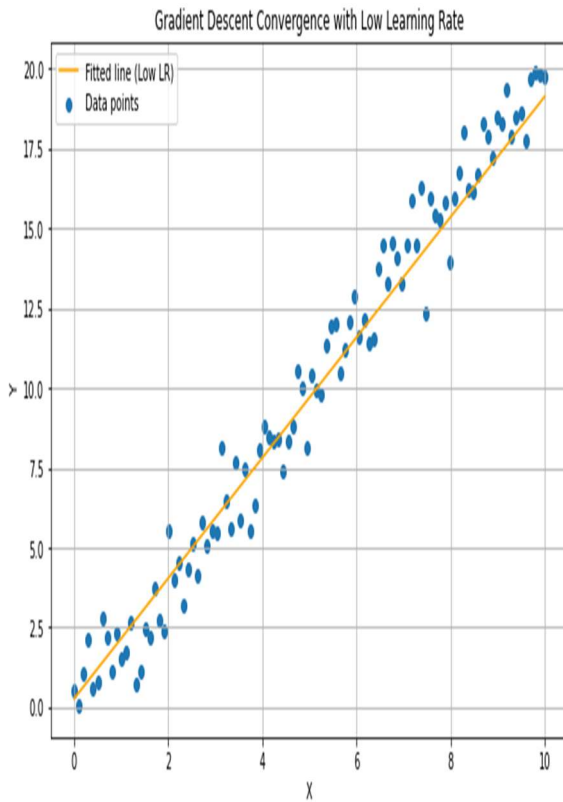


Figure 20. Gradient Descent Convergence Plot With Low Learning Rate

The convergence plot for Stochastic Gradient Descent with mini-batch sampling has been projected as shown in Figure 21. The purple line represents the fitted line by the Stochastic Gradient

Descent algorithm with mini-batch sampling. The convergence plot allows researchers to analyze the convergence rate of SGD with mini-batch sampling. They can observe whether the algorithm converges quickly to a satisfactory solution or requires additional iterations to reach convergence.

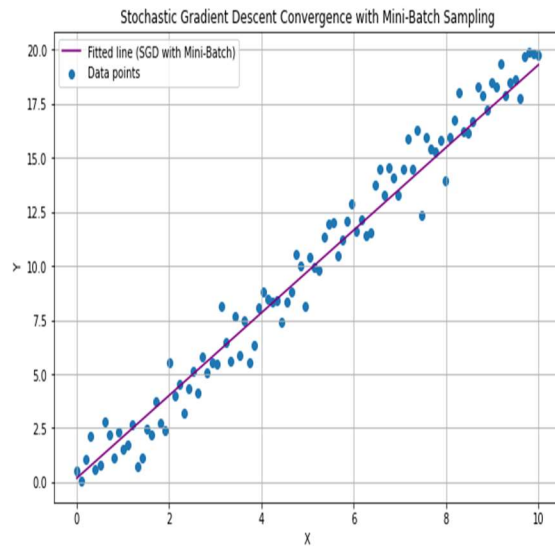


Figure 21. Stochastic Gradient Descent Convergence Plot With Mini Batch Sampling

In our enhanced study, the convergence plot for Gradient Descent with momentum was projected as shown in Figure 22. The purple line represents the fitted line by the Gradient Descent algorithm with momentum. Researchers can compare the convergence rates of Gradient Descent with momentum and standard Gradient Descent. By analyzing the steepness of the convergence curves, they can assess whether momentum accelerates convergence and improves optimization efficiency.

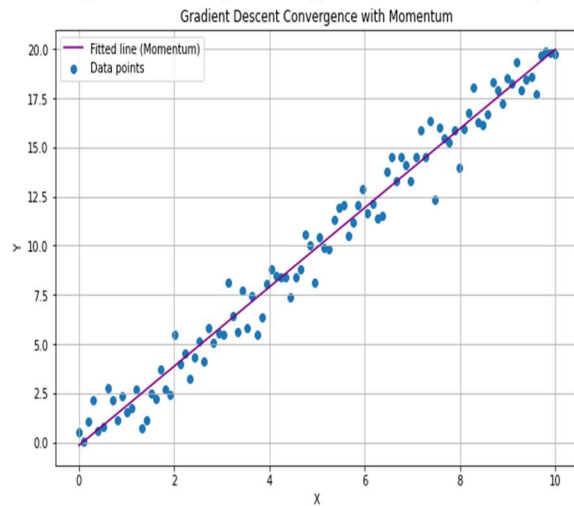


Figure 22. Convergence Plot For Gradient Descent With Momentum

Table. 7 Comparative Study And Unintended Outcomes

Aspect	Current Study	Previous Literature	Unintended Outcomes
Optimization Technique	Pareto Multi-Objective Genetic Algorithm (PMOGA)	Classical methods, heuristic algorithms	Increased computational complexity and time for convergence
Side Lobe Level (SLL)	Reduced from -17.41 dB to -24.84 dB	Typically higher SLL with classical designs (~-15 to -18 dB)	Potential trade-offs in beamwidth or other performance aspects
Number of Elements	Reduced from 341 to 220	No significant reduction in elements achieved previously	Limited reduction in element count may impact design flexibility
Array Efficiency (η)	Achieved 64.9%	Often less efficient with classical methods (~50-60%)	Higher efficiency might come with increased algorithm complexity
Half Power Beam Width	Comparable to fully populated array	Varies; often broader in non-optimized designs	Minor discrepancies in beamwidth might occur during optimization
Computational Complexity	Increased due to PMOGA's complexity	Lower with classical methods but less optimization capability	Higher computational cost might affect practical implementation

CONTEXT IN CURRENT INDUSTRY SCENARIO:

Enhanced performance: The ability to reduce side lobe levels while minimizing the number of antenna elements addresses key performance issues in mobile and satellite communication systems. Improved SLL leads to reduced interference and better signal quality, which is crucial for high-performance communication applications.

Cost Efficiency: By thinning the antenna array and reducing the number of elements from 341 to 220, significant cost savings can be achieved in terms of manufacturing, deployment, and maintenance. This reduction can make advanced antenna technologies more economically viable and accessible.

Implementation Feasibility: The optimized array design with PMOGA ensures that the practical implementation of the antenna system remains efficient. The close match in half power beam width with the fully populated array ensures that the performance characteristics are preserved, facilitating easier integration into existing communication infrastructure.

5. CONCLUSION

The application of the Pareto Multi-Objective Genetic Algorithm (PMOGA) has proven to be highly effective for optimizing the thinning of large concentric ring antenna arrays composed of isotropic elements. This research successfully demonstrates that PMOGA can achieve a significant reduction in the number of elements while maintaining high array efficiency ($\eta = 64.9\%$) and improving side lobe levels (SLL) from -17.41 dB to -24.84 dB. Additionally, the synthesized array pattern retains a half power beam width comparable to that of the fully populated array, ensuring that key performance characteristics are preserved. These findings highlight the potential of evolutionary optimization techniques to address the challenges of antenna array design, offering substantial improvements in both efficiency and performance. The results are consistent with the study's objectives and provide valuable insights for advancing the state-of-the-art in antenna technology for mobile and satellite communication systems. This work not only contributes to theoretical advancements but also offers practical

solutions for optimizing antenna arrays in real-world applications.

REFERENCES

- [1] CABalanis, "Antenna Theory: analysis and design, 3rd edition, John Wiley& Sons, New York, 2005
- [2] R L. Haupt, "Optimized element spacing for low side lobe concentric ring arrays," IEEE Transactions on Antennas and Propagation, vol. 56, no. 1, 2008, pp. 266–268.
- [3] Haupt, Thinned concentric ring arrays, IEEE Transactions on Antennas and Propagation, 2008.
- [4] Sherman, MISkolone, Thinning planar array antennas with ring arrays, 1958 IRE International Convention Record, vol.11, 1963, 77-86.
- [5] K. Choi, D. Jang, S. Kang, J. Lee, T. Chung and H. Kim, Hybrid Algorithm Combing Genetic Algorithm with Evolution Strategy for Antenna Design, IEEE Transactions on Magnetics, vol. 52, no. 3, March 2016, pp. 1-4.
- [6] F. Bin, F. Wang, S. Chen, Q. Sun, L. Zhong and S. Lin, Pareto-optimal design of UHF antenna using modified non-dominated sorting genetic algorithm II, IET Microwaves, Antennas & Propagation, vol. 14, no. 12, 2020, pp. 1404-1410.
- [7] J. S. Smith and M. E. Baginski, Thin-Wire Antenna Design Using a Novel Branching Scheme and Genetic Algorithm Optimization, IEEE Transactions on Antennas and Propagation, vol. 67, no. 5, May 2019 pp. 2934-2941.
- [8] S. Mosca, M. Ciattaglia, Ant Colony Optimization to Design Thinned Arrays, IEEE, 2006.
- [9] DMandal HKumar SPGhosal RKar, Thinned concentric circular antenna array synthesis using particle swarm optimization, Proceedia technology, ELSEVIER, 6, 2012, 848-855.
- [10] Lakshman Pappula, Gosh, Linear antenna array synthesis using cat swarm optimization, International Journal of Electronics and Communications, 99(3), 2018, 1169-1194.
- [11] Singh, A., Mehra, R. M., & Pandey, A Hybrid Approach for Antenna Optimization Using Cat Swarm based Genetic Optimization, Advanced Electromagnetics, 7(3), 2018, 23-34.
- [12] Babayigit, B, Synthesis of concentric circular antenna arrays using dragonfly algorithm, International Journal of Electronics, 105(5), 2018, 784-793.
- [13] Sun, G., Liu, Y., Li, H., Liang, S., Wang, A., & Li , An Antenna Array Side lobe Level Reduction Approach through Invasive Weed Optimization, International Journal of Antennas and Propagation, 2018.
- [14] Li, W. T., Hei, Y. Q., & Shi, X. W, Synthesis of Conformal Phased Antenna Arrays with A Novel Multiobjective Invasive Weed Optimization Algorithm, Frequenz, 72(5-6), 2018, 209-219.
- [15] Zhang, C., Fu, X., Lighthart, L. P., Peng, S., & Xie, M, Synthesis of Broadside Linear A periodic Arrays with Side lobe Suppression and Null Steering Using Whale Optimization Algorithm, IEEE Antennas and Wireless Propagation Letters, 17(2), 2018, 347-350.
- [16] Zhang, C., Fu, X., Peng, S., & Wang, Y, Linear unequally spaced array synthesis for side lobe suppression with different aperture constraints using whale optimization algorithm, IEEE Conference on Industrial Electronics and Applications (ICIEA) , May 2018 ,pp. 69-73.
- [17] M.gopiSridhar, k v satyanarayana, Interference suppression in wireless communications by adaptive beam forming algorithm and windows, International Journal of Engineering and Advanced Technology , Vol.8 Issue-3, Feb 2019.
- [18] Darvish, A., & Ebrahimzadeh, A, Improved Fruit-Fly Optimization Algorithm and Its Applications in Antenna Arrays Synthesis, IEEE Transactions on Antennas and Propagation, 66(4), 2018, 1756-1766.
- [19] Polo-Lopez, L., Córcoles, J., & Ruiz-Cruz, J. A, Antenna Design by Means of the Fruit Fly Optimization Algorithm, Electronics, 7(1), 2018.
- [20] Sanjaykumar Dubey, Debasis Mandal, Akhilesh kumar Mishra, Highly Directive Array Pattern Synthesis in Different phi planes of a Large Concentric circular ring antenna array (CCRAA) using Array Thinning Technique, Advanced Electromagnetics, vol 11, No 2, 2022.
- [21] Geng Sun, Yanheng Liu, Zhaoyu Chen, Shuang Liang, Aimin Wang, and Ying Zhang, Radiation Beam Pattern Synthesis of Concentric Circular Antenna Arrays Using Hybrid Approach Based on Cuckoo Search, IEEE Transactions on Antennas and Propagation. Vol 66, Issue 9, 2018.
- [22] Xujian wang, minliyao, fenggan zhang, dinghengdai, Synthesis of sparse concentric ring arrays based on fitness –associated differential evolution algorithm, International journal of antennas and propagation, 2019.